UNVEILING URBAN AIR QUALITY SEASONAL DYNAMICS IN SAN MIGUEL DE TUCUMÁN, ARGENTINA, BY SCANNING ELECTRON MICROSCOPY

Enzo Rubén Marcial[1,2,3], Alexander Aldo Santucho Cainzo[4], Facundo Reynoso Posse[2,5], Rodrigo Gastón Gibilisco[2], Aida Ben Altabef[2], Diego Hernando Corregidor Carrió[4], Virginia Helena Albarracín[1,3*]

[1]Centro Integral de Microscopía Electrónica (CIME-UNT-CONICET), Facultad de Agronomía, Zootecnia y Veterinaria, Universidad Nacional de Tucumán, Camino de Sirga s/n, Yerba Buena, Tucumán, 4107, Argentina.

[2]Laboratorio de Estudios Atmosféricos (LEA), Instituto de Química del Noroeste, INQUINOA-CONICET-Universidad Nacional de Tucumán, San Lorenzo 456, Tucumán, 4000, Argentina.

[3]Facultad de Ciencias Naturales e IML, Universidad Nacional de Tucumán, Miguel Lillo 205, Tucumán, 4000, Argentina.

[4]Instituto de Luz, Ambiente y Visión (ILAV), Universidad Nacional de Tucumán, Av. Independencia 1701, Tucumán, Argentina.

[5]Instituto de Altos Estudios Espaciales Mario Gulich, Universidad Nacional de Córdoba, Ruta C45 Km 8, Falda del Cañete, Córdoba, Argentina.

*Corresponding author. Dr. Virginia Helena Albarracín, Centro Integral de Microscopía Electrónica (CIME-UNT-CONICET), Finca El Manantial UNT, Facultad de Agronomía, Zootecnia y Veterinaria; Camino de Sirga s/n (4107), Yerba Buena, Tucumán, Argentina. E-mail: valbarracin@csnat.unt.edu.ar

ABSTRACT

Scanning Electron Microscopy (SEM) coupled with Energy Dispersive X-ray Spectroscopy (EDS) was used to analyze particulate matter (PM) in San Miguel de Tucumán, Argentina, a densely populated urban area influenced by agricultural and industrial pollution. This study investigates PM concentration and composition during sugarcane harvest and non-harvest periods (2019-2020), accidentally coinciding with the COVID-19 lockdowns. SEM-EDS enabled the classification of PM by size (Dust, PM_{10}, and $PM_{2.5}$) and by composition (Terrigenous PM and Carbonaceous PM). Higher PM concentrations were detected during harvest periods, with a notable increase in carbon-rich $PM_{2.5}$ ($PMC_{2.5}$) in 2019 compared to 2020. Unexpectedly, this variation was primarily attributed to reduced population mobility during the 2020 lockdowns, rather than changes in industrial activity. Satellite data on nitrogen oxides (NOx) supported these findings, revealing emission patterns consistent with vehicular activity. Overall, this study demonstrates the effectiveness of SEM-EDS in characterizing air pollutants and highlights the critical influence of population mobility on urban air quality. The findings support the implementation of targeted air pollution control strategies - particularly during harvest seasons- to mitigate both health and environmental impacts.

Keywords: Particulate matter, SEM, EDS, Air quality.

1. Introduction

Air pollution poses a major threat to urban environments, particularly in regions where agricultural and industrial activities coexist. Particulate matter (PM), a complex mixture of solid particles and liquid droplets suspended in the air, is a key contributor to degraded air quality, with significant health and environmental consequences (Ministry of Environment and Sustainable Development, 2021**;** World Health Organization, 2021). The city of San Miguel de Tucumán, Argentina, exemplifies these challenges, being a densely populated urban center surrounded by intensive agricultural operations, notably sugarcane farming, which substantially influences seasonal air pollution patterns.

PM is commonly classified according to aerodynamic diameter into Dust (>10 µm), PM_{10} (<10 µm), and $PM_{2.5}$ (<2.5 µm), each posing specific health risks (Pakbin et al., 2010). Exposure to PM has been associated with a wide range of diseases, including respiratory, cardiovascular, and neurological disorders, as well as increased mortality (Correia et al., 2013**;** World Health Organization, 2021). In Tucumán, seasonal practices such as sugarcane field burning—despite being legally prohibited by Provincial Law No. 6253, Art. 38—continue to exacerbate air quality problems, contributing to peaks in respiratory and ocular conditions (Altieri et al., 2018; Jordán and Flores, 2018).

PM originates from diverse sources, including industrial activities, vehicular emissions, biomass burning, and agricultural residues. Key components of PM include sulfates, nitrates, ammonia, sodium chloride, mineral dust, ashes, and carbonaceous particles. Carbonaceous particles, forming 20–45% of fine particles, are primarily released through combustion processes, such as biomass and agricultural residue burning (Ji et al., 2016**;** Dinoi et al., 2017). These particles significantly impair air quality, not only by increasing light absorption in the atmosphere but also by reducing visibility (Zhou et al., 2012; Bisht et al., 2016; Lee et al., 2017), which is one of the most perceptible consequences of atmospheric pollution. The use of organic tracers has identified primary sources of elemental carbon, including coal combustion, vehicle exhaust, biomass burning, and vegetative detritus (Li et al., 2013). In Tucumán, the seasonal burning of sugarcane fields intensifies PM concentrations, complicating air quality management efforts. Although this practice is prohibited by Provincial Law No. 6253, Art. 38, enforcement remains limited, and comprehensive regulations to mitigate air pollution are lacking.

Current air quality monitoring systems in Tucumán, and worldwide, are constrained by technological and methodological limitations, with yet scarce development of innovative, cost-

effective analytical techniques. Traditional methods such as gravimetric analysis (Almeida et al., 2006; Chatoutsidou and Lizariadis, 2022) and optical particle counters (Wang et al., 2021, Mills et al., 2024) are widely used but often lack the precision needed to determine the chemical composition of PM or require expensive, specialized equipment. Scanning Electron Microscopy (SEM) coupled with Energy-Dispersive X-ray Spectroscopy (EDS) offers a robust alternative for PM characterization, providing high-resolution insights into particle size, morphology, and chemical composition, this way, it is possible to identify individual particles originating from specific sources such as coal mines, road wear, brakes and wheels, sea salt, soil, and industries(Casuccio et al., 2004;Fanizza et al., 2018; Rausch et al., 2022; Li et al., 2023; Zhao et al., 2023; Aubourg et al., 2024). Despite its potential, SEM-EDS remains an underexploited tool in the context of regional air quality studies.

In this context, the present study explores how seasonal agricultural practices, coupled with variations in human activity, influence the concentration, size distribution, and chemical composition of PM in an urban environment. By applying SEM-EDS to samples collected across harvest and non-harvest seasons—and coinciding with the exceptional conditions imposed by COVID-19 lockdowns—this work aims to elucidate the relative contributions of natural and anthropogenic factors to particulate pollution in San Miguel de Tucumán. Ultimately, the findings are intended to support the development of targeted air quality management strategies in urban areas impacted by agricultural activities.

2. Methods

2.1.Sampling Design and Collection

Samples were collected at the Quinta Agronómica campus of the National University of Tucumán, located in central-southern San Miguel de Tucumán. An open field was chosen to minimize contamination from nearby trees and buildings.

The sampling device used adhesive carbon tape—which retains settled particles—mounted on an aluminum stub and fixed to a polystyrene base for stability and easy removal (Figure 1). It was placed at a height of 2 meters and stored in airtight glass containers to prevent contamination during transport.

Sampling occurred weekly from August 2019 to August 2020, between 07:00 and 19:00. Rainy days were avoided to prevent interference from precipitation. Sampling paused in January (university recess) and mid-March to mid-April due to the COVID-19 lockdown. Preliminary tests showed that the adhesive surface was effective for up to 36 hours of exposure.

2.2.PM Characterization Using SEM

Samples were imaged using a Zeiss Supra 55VP microscope at the Centro Integral de Microscopía Electrónica (CIME, CONICET-UNT). SEM provided three-dimensional images of the sample surface with superior depth of field and detail compared to conventional optical microscopy. This enabled detailed imaging and analysis of particles within the micrometer scale.

Images were acquired using backscattered electrons at 15 kV, a working distance of 8 mm, and an aperture of 60 µm. High-resolution images (3072 × 2304 pixels) were captured at 300x magnification, allowing the analysis of particles with diverse diameters.

2.3.Chemical Analysis of PM Using EDS

The chemical composition of individual particles was analyzed using an X-ray spectrometer coupled to the SEM. At least 300 particles were randomly selected and analyzed based on grayscale differences in SEM images. EDS spectra were acquired using Oxford INCA EDS, with the electron beam positioned at the particle center for precise compositional data.

2.4.Image Processing and Analysis

SEM images were processed using the free-access software ImageJ® (National Institutes of Health, https://imagej.nih.gov/ij/index.html). Approximately 15,000 particles distributed over the year of sampling were peaked in the SEM images and subjected to image analysis. This allows us to estimate PM concentration levels during the sampling period through particle number measure in a standardized number of microphotographs. Images were scaled by setting a pixel-to-distance measure based on the SEM's magnification settings. Cropping was applied to exclude parameter bars, and normalization adjusted the background grayscale value to a uniform level of 30. Profile values were plotted, taken along transects that included carbon-rich particles, silica-rich particles, and background to observe limit pixel values between particles and background (Figure 2). This method helped to standardize analysis of SEM images for particle characterization and comparison.

Thresholding was employed to differentiate particles from the background, setting a pixel value range of 50–255 for particles (Figure 3a). Noise and imperfections on the carbon tape were corrected using the "Brush" tool and a median filter. Particle parameters, including area, mean gray value, Feret diameters (maximum and minimum), circularity, and roundness, were measured using the "Analyze Particles" command on the normalized images (Figure 3b).

Parameters obtained with ImageJ, such as Feret diameters, were used to calculate the equivalent diameter (D_{eq}) of individual particles (Merkus, 2009; Sgrigna et al., 2016). Particles were then classified into three distinct categories based on D_{eq}: I) Dust: Particles >10 µm; ii) PM_{10}: Particles <10 µm and >2.5 µm; $PM_{2.5}$: Particles <2.5 µm.

Ultra-fine particles, such as PM_1 (<1 µm), were excluded from the analysis for two reasons: i) these particles remain suspended in the air and are less likely to settle on the adhesive surface unless direct contact occurs, and ii) their small size results in higher measurement errors, even with optimal resolution.

For each sample, 12 images were analyzed, and the resulting data were unified using the statistical programming language "R" (https://www.r-project.org/) to facilitate comparison across samples.

2.5.Environmental Parameter Analysis

Meteorological data, including temperature, relative humidity, and wind speed, were obtained from the National Meteorological System of Argentina (https://www.argentina.gob.ar/smn). Correlations between these parameters and PM distribution were assessed using Spearman correlation coefficients (ρ) calculated with R, which provided insights into the direction and intensity of these relationships.

2.6. Nitrogen oxides mapping

For comparison with PM data, concentration and distribution maps of nitrogen oxides (NO_2) were generated using QGIS 3.34 software (https://qgis.org/project/visual-changelogs/visualchangelog334/). Sentinel-5P satellite products were obtained from the Sentinel Hub repository via the EO Browser platform (https://apps.sentinel-hub.com/eo-browser). The selected products had been pre-processed by the provider for nitrogen dioxide (NO_2), using the S5P/TROPOMI NO_2 version 2.2.0 dataset, which offers improved sensitivity to these gases and reports their tropospheric column density in mol/m². Only satellite images corresponding to dates

without cloud interference were selected. For both 2019 and 2020, the days with the highest and lowest $PMC_{2.5}$ concentrations during the sugarcane harvest season were analyzed, only if the corresponding satellite data were available. For spatial analysis, a study area with a 20 km radius centered on the sampling site was used, extending radially to the boundaries of San Miguel de Tucumán.

3. Results

3.1. Quantification of PM and Size Distribution Using SEM Image Analysis

SEM image analysis revealed seasonal patterns in PM levels throughout the 2019–2020 period (Supplementary File available at 10.5281/zenodo.15520804). Peaks occurred in August and September, during sugarcane harvest, likely due to biomass burning article counts decreased during wetter and warmer months (December to March), confirming the influence of climatic conditions. The COVID-19 lockdown (March to November 2020) also affected PM levels.

During harvest season, PM concentrations increased by 110% in 2019 and 163% in 2020, compared to non-harvest months. Average PM counts were 695 particles/sample in 2019 and 870 particles/sample in 2020, versus 331 particles/sample outside harvest periods (Figure 4). This aligns well with findings from industrial cities, where PM_{10} and $PM_{2.5}$ concentrations were found to be up to 2.0 and 1.7 times higher than national standards due to industrial and vehicular emissions (Xu et al., 2019).

Dust, PM_{10}, and $PM_{2.5}$ levels were highest during harvest season (Figure 5). In 2019, finer particles (PM_{10} and $PM_{2.5}$) dominated, suggesting combustion sources. In contrast, in 2020, all size fractions increased more uniformly, highlighting the influence of multiple PM sources and meteorological effects on particle distribution.

3.2. Chemical Composition and Classification of PM

EDS analysis identified consistent elemental composition across the sampled particles, with predominant elements being carbon (54.3%), silicon (26.13%), aluminum (4.82%), potassium (3.90%), calcium (2.73%), and iron (2.82%). This enabled classification into two main groups: i) Carbonaceous Particulate Matter (PMC): predominantly composed of carbon, associated with "black carbon" or "total carbon" from biomass burning and combustion (Shen et al., 2021); and

ii) Terrigenous Particulate Matter (PMT): composed primarily of silicon, aluminum, potassium, calcium, and iron, characteristic of "soil dust" or "mineral dust," typically derived from rock and soil-forming minerals(Camino *et al.*, 2015; Hosseini and Shahbazi, 2016).

The mean gray value of SEM images served as an indicator of chemical composition, enabling the discrimination between PMC (gray values of 30–100) and PMT (gray values >100). This approach facilitated the analysis of particle distribution and compositional variability, revealing a clear dominance of PMT over PMC throughout the year (Figure 6a and 6b), except in $PM_{2.5}$, fraction, which exhibited a high concentration on PMC (Figure 6c). Compared with the non-harvest season there is an average increase of 92% for DustT, 103% for PMT_{10} and 211% for $PMT_{2.5}$ during harvest season of 2019, and 207% for DustT, 171% for PMT_{10} and 253% for $PMT_{2.5}$ during harvest season of 2020. A similar pattern was observed for PMC, the increase is 119% for DustC, 70% for PMC_{10} and 144% for $PMC_{2.5}$ during harvest season of 2019, and 49% for DustC, 42% for PMC_{10} and 103% for $PMC_{2.5}$ during harvest season of 2020.PMTwas more abundant, likely due to drier soil conditions and wind erosion, suggesting that environmental conditions could play a crucial role in PM size composition and distribution (Yadav et al., 2017). The high content of PMC in finer particles could be explained by increased combustion activity, either from biomass burning or fossil fuel combustion, as reflected in $PMC_{2.5}$ levels (Grange et al., 2022; Paisi et al., 2024).

3.3. Environmental Influences on PM

Environmental parameters such as humidity, wind speed, and temperature influenced PM transport and deposition (Figure 7), as evidenced by the Spearman correlation coefficient (ρ). In this case, humidity was negatively correlated with PM (ρ=−0.572), indicating particle settling during high humidity. Likewise, wind speed showed a positive correlation (ρ=0.398), suggesting the resuspension of particles from surrounding surfaces under windy conditions. Lastly, temperature exhibited a negative correlation (ρ=−0.386), potentially reflecting increased particle deposition during periods of high humidity and temperature.

These findings highlight the importance of meteorological factors in PM dynamics. Wind erosion appears to be a significant driver of PMT levels, while humidity plays a key role in reducing airborne PM through wet deposition. That is why during dry season, coinciding with harvest period, the presence of PMT in the air of San Miguel de Tucumán is higher than wet or

non-harvest season. This behavior is similar to that observed by Yadav et al. (2017,) described in India during monsoon season, and Zalakeviciute et al. (2020) in Ecuador during the transition between dry and wet seasons.

3.4. Sugarcane Burning and PMC Contributions

The anthropogenic activities also contribute to the presence of PM in the air of San Miguel de Tucumán. Finer PMC generally comes from combustion processes like biomass burning and fossil fuel combustion (Grange et al., 2022; Paisi et al., 2024). In this case the most relevant source of biomass burning, originates from the important industrial activity in Tucumán province, the sugar industry (García et al., 2018). Sugar cane fields burning is a significant contributor to $PMC_{2.5}$ to the air. As mentioned in section 3.3, the PMC increase during sugarcane harvest season but the size range more abundant is the $PMC_{2.5}$, with an average ratio $PMC_{2.5}$:$PMT_{2.5}$ of 1:0.9 in the year 2019 and 1:1.2 in the year 2020 (Figure 6c).This would indicate that there was more contribution of biomass burning during the year 2019 than the year 2020, but according to the survey of burned areas in the productive area of the province of Tucumán during the 2020 crop season done by the Estacion Experimental Agroindustrial Obispo Colombres (EEAOC, 2020), there were more surface burned during 2020, 61.000 ha more than 2019. This shows that even though biomass burning is an important source of $PMC_{2.5}$, there is another one to be considered: the fossil fuel combustion associated with vehicle fleet, it was providing more particles in 2019 than 2020.

3.5. Influence of Population Mobility and NOx

The decrease of $PMC_{2.5}$ from 2019 to 2020 is interpreted as a direct result diminution of combustion vehicles circulating around the sampling zone and in all San Miguel de Tucumán, due to COVID-19 lock down, during the year 2020. One of the main contributions of fossil fuel combustion to the air is fine $PMC_{2.5}$ (Grange et al., 2022; Paisi et al., 2024). The lockdown significantly reduced population mobility, as shown in the Google Mobility Report (https://www.google.com/covid19/mobility/?hl=es) for the region of San Miguel de Tucumán, therefore it also reduced $PMC_{2.5}$.

To support this hypothesis, data from satellite-derived nitrogen oxides (NO_x) distribution maps were used (Figure 8). NO_x is considered as one of the criteria pollutants according to the United States Environmental Protection Agency (EPA). Includes gases such as NO_2 and NO, highly reactive gases that primarily come from the burning of fuel. The analysis made considered dates where peaks in $PMC_{2.5}$ concentration were observed in the study area as well as days with lower $PMC_{2.5}$ concentrations. The distribution of NO_x gases shows that concentration of this gas was high during the peak of $PMC_{2.5}$ in 2019 (Figure 8a), while it decreased on dates when $PMC_{2.5}$ was lower (Figure 8b). In 2020, this pattern remained consistent for both pollutants (Figure 8c and 8d); however, when comparing the two years, it is observed that pollution levels in 2020 were lower than in 2019. These results show that NO_x concentration decreased in 2020, corresponding to the period when both population mobility and $PMC_{2.5}$ concentration declined. Additionally, the NO_x concentration observed in 2019 could be considered a reference or 'normal' value for a year without confinement measures, which again aligns with the high $PMC_{2.5}$ concentration, supporting the role of traffic emissions in $PMC_{2.5}$ presence.

4. Discussion

The results of this study highlight the complex interplay between seasonal agricultural practices, industrial activity, urban mobility, and atmospheric conditions in shaping air quality in San Miguel de Tucumán. The increase in $PM_{2.5}$ concentrations during the sugarcane harvest season aligns with previous research linking biomass burning to elevated fine particulate levels in South American cities (Mendez-Espinosa et al., 2019). However, the observed decline in $PMC_{2.5}$ in 2020 -despite a larger burned area- suggests that vehicular traffic contributes more substantially to carbonaceous fine particles than previously acknowledged. This is consistent with findings from urban environments in Europe and Asia, where traffic emissions dominate $PM_{2.5}$ sources (Grange et al., 2022; Tessum et al., 2022; Liao et al., 2023; Paisi et al., 2024). This is further supported by the positive correlation between NOx satellite data and $PMC_{2.5}$ levels, reinforcing the role of human mobility in combustion-related emissions.

These insights support the growing consensus that integrated monitoring strategies—including high-resolution morphological and chemical analyses—are essential for understanding urban air pollution dynamics and designing targeted mitigation policies (Baldacchini et al., 2019; Chen et al., 2022). In this context, SEM-EDS emerged as a scalable and precise tool for PM source

apportionment, especially in mid-sized cities where conventional monitoring networks are limited.

By analyzing over 15,000 particles collected in one year, we identified significant temporal and compositional variability in PM related to anthropogenic activities such as sugarcane burning and traffic, modulated by meteorological factors. SEM-EDS enabled the classification of particles into carbonaceous (PMC) and terrigenous (PMT) fractions, providing insights into seasonal emission sources. Its capacity to integrate morphology and elemental composition at the microscale proved critical for source attribution under complex atmospheric conditions (Martínez Morales et al., 2023; Pandey and Negi, 2022).

The COVID-19 lockdown offered a unique opportunity to disentangle the effects of reduced human activity. Our results revealed a strong association between reduced traffic and lower $PMC_{2.5}$ levels, consistent with findings from other regions where mobility restrictions led to significant decreases in $PM_{2.5}$ levels (Arregocés et al., 2021; Martínez Morales et al., 2023). However, other studies have highlighted that such reductions are not always straightforward. For instance, Zangari et al. (2020) reported that changes in PM levels during the lockdown period were within the range of interannual variability, suggesting that natural variability and meteorological conditions also play a role. Pandey and Negi (2022) found that biomass burning was the primary contributor to PM during lockdowns in their study area, underscoring the regional specificity of emission sources. Similarly, Speranza and Caggiano (2022) further noted that pandemic-related mobility restrictions affected both coarse and fine PM fractions differently across study sites, indicating that the impact of lockdowns on PM composition is spatially heterogeneous. Post-pandemic analyses, such as Qonitan et al. (2023) in Jakarta, Indonesia, showed a deterioration in air quality linked to vehicular and coal combustion emissions. Taken together, these findings reinforce the value of SEM-EDS as a diagnostic tool for particle classification and for understanding the multifactorial nature of air pollution, especially under abrupt changes in human activity such as those caused by the COVID-19 pandemic.

A major advantage of SEM-EDS lies in its ability to bridge the gap between high-precision laboratory techniques and real-time monitoring, offering a benchmark for calibrating low-cost air quality sensors. The method's ability to combine morphological and chemical information enhances its relevance in urban settings with complex emission profiles.

Ultimately, the findings of this study not only demonstrate the potential of SEM-EDS in air quality research but also highlight critical intervention points for environmental policy. In

particular, the seasonal impact of agricultural burning and vehicular emissions on urban PM levels urges the need for stricter enforcement of burning bans, improved traffic regulation, and targeted air pollution mitigation strategies in Tucumán and other regions facing similar challenges. Most importantly, our objective goes beyond characterizing air quality: we aim to promote this issue as an urgent public health and environmental challenge. By providing high-resolution data on pollution sources, we seek to empower evidence-based policymaking and emphasize the necessity of strengthening local and regional frameworks to ensure more effective public health protection and long-term sustainable urban development.

Credit authorship contribution statement

Enzo Rubén Marcial: Conceptualization, Investigation, Methodology, Formal analysis, Validation, Visualization, Writing – original draft. **Alexander Aldo Santucho Cainzo:** Methodology. **Facundo Reynoso Posse:** Investigation, Visualization. **Rodrigo Gastón Gibilisco:** Review& editing; **Aida Ben Altabef**: Review & editing. **Diego Hernando Corregidor Carrió:** Formal Analysis, Investigation, Resources, Supervision, Project administration, review & editing. **Virginia Helena Albarracín:** Funding acquisition, Investigation, Resources, Supervision, Project administration, Writing – review & editing.

Acknowledgments

The authors acknowledge the generous financial support by the National Council of Research and Technology (CONICET) and ex Ministry of Science, Technology and Innovation of Argentina (MINCyT) through “Programa de Articulación y Fortalecimiento Federal de las Capacidades en Ciencia y Tecnología COVID□19”. This work was funding by the Project TUC□03□COVID19 “COVID□U□MAP”, included in the Bank of Technological and Social Development Projects of CONICET (PDTS). Our group was part of the “Federal Network for COVID detection in the environment”, Unidad Coronavirus, MINCyT. The Project received financial support of the Provincial Health Ministry in the frame of COVID□19 Research Program, processed by a specific agreement between the Superior Government of the Province of Tucumán, the National University of Tucumán and CONICET. ERM is a postdoctoral researcher from CONICET. VHA, RGG, ABA are staff researchers and DHCC and staff technicians. VHA was a recipient of a Georg Foster Scholarship for Experienced Researchers, Alexander von

Humboldt Foundation (2021-2023) and of a grant of the Williams Foundation (Fondos Complementarios para Proyectos con Impacto en el Territorio 2024). We would also like to thank technical assistance of Luciano Martinez and Hernán Esquivel for imaging samples. All micrographs and EDS data were taken at the Centro Integral de Microscopía Electrónica (CIME), belonging to UNT and CONICET, in Tucumán, Argentina.

Declaration of Competing Interest

The authors declare that they have no known competing financial interests or personal relationships that could have appeared to influence the work reported in this paper.

References

Almeida, S.M., Pio, C.A., Freitas, M.C., Reis, M.A., Trancoso, M.A., 2006. Approaching $PM_{2.5}$ and $PM_{2.5-10}$ source apportionment by mass balance analysis, principal component analysis and particle size distribution. Sci. Total Environ.368(2-3), 663-674. https://doi.org/10.1016/j.scitotenv.2006.03.031.

Altieri, H.H., Bruno, M.E., Calli, R., Ríos, V.H., Meoni, G.S., 2018. Prevalencia de síntomas respiratorios y oculares en época de zafra en escolares de una ciudad de Tucumán, en relación con la contaminación ambiental 2010-2012. https://msptucuman.gov.ar/wordpress/wp-content/uploads/2019/02/revista-cientifica-4-para-web.pdf.

Arregocés, H.A., Rojano, R., Restrepo, G., 2021. Impact of lockdown on particulate matter concentrations in Colombia during the COVID-19 pandemic. Sci. Total Environ. 764, 142874. https://doi.org/10.1016/j.scitotenv.2020.142874

Aubourg, M.A., Livi, K.J.T., Sawtell, G.G., Sanchez-Gonzalez, C.C., Spada, N.J., Dickerson, R.R., Chiou, W.A., Kamazi, C., Ramachandran, G., Rule, A.M., Heaney, C.D., 2024. Use of electron microscopy to determine presence of coal dust in a neighborhood bordering an open-air coal terminal in Curtis Bay, Baltimore, Maryland, USA. Sci. Total Environ. 957, 176842. https://doi.org/10.1016/j.scitotenv.2024.176842.

Baldacchini, C., Sgrigna, G., Clarke, W., Tallis, M., Calfapietra, C., 2019. An ultra-spatially resolved method to quali-quantitative monitor particulate matter in urban environment. Environ. Sci. Pollut. Res. 26, 18719-18729. https://doi.org/10.1007/s11356-019-05160-8.

Bisht, D.S., Tiwari, S., Dumka, U.C., Srivastava, A.K., Safai, P.D., Ghude, S.D., Chate, D.M., Rao, P.S.P., Ali, K., Prabhakaran, T., Panickar, A.S., Soni, V.K., Attri, S.D., Tunved, P., Chakrabarty, R.K., Hopke, P.K., 2016. Tethered balloon-born and ground-based measurements of black carbon and particulate profiles within the lower troposphere during the foggy period in Delhi, India. Sci. Total Environ. 573, 894–905. https://doi.org/10.1016/j.scitotenv.2016.08.185.

Camino, C., Cuevas, E., Basart, S., Alonso-Pérez, S., Baldasano, J.M., Terradellas, E., Marticorena, B., Rodríguez, S., Berjón, A., 2015. An empirical equation to estimate mineral dust concentrations from visibility observations in Northern Africa. Aeolian Res. 16, 55-68. https://doi.org/10.1016/j.aeolia.2014.11.002.

Casuccio, G.S., Schlaegle, S.F., Lersch, T.L., Huffman, G.P., Chen, Y., Shah, N., 2004. Measurement of fine particulate matter using electron microscopy techniques. Fuel process. Technol. 85(6-7), 763-779. https://doi.org/10.1016/j.fuproc.2003.11.026.

Chatoutsidou, S.E., Lazaridis, M., 2022. Mass concentrations and elemental analysis of $PM_{2.5}$ and PM_{10} in a coastal Mediterranean site: A holistic approach to identify contributing sources and varying factors. Sci. Total Environ. 838, 155980. https://doi.org/10.1016/j.scitotenv.2022.155980.

Chen, H.S., Lin, Y.C., Chiueh, P.T., 2022. High-resolution spatial analysis for the air quality regulation service from urban vegetation: A case study of Taipei City. Sustain. Cities Soc. 83, 103976. https://doi.org/10.1016/j.scs.2022.103976.

Correia, A.W., Pope, C.A.III, Dockery, D.W., Wang, Y., Ezzati, M., Dominici, F., 2013.Effect of air pollution control on life expectancy in the United States: An analysis of 545 US counties for the period 2000 to 2007. Epidemiol. 24,23. 10.1097/EDE.0b013e3182770237.

Dinoi, A., Cesari, D., Marinoni, A., Bonasoni, P., Riccio, A., Chianese, E., Tirimberio, G., Naccarato, A., Sprovieri, F., Andreoli, V., Moretti, S., Gullí, D., Calidonna, C.R., Ammoscato, I., Contini, D., 2017. Inter-comparison of carbon content in $PM_{2.5}$ and PM_{10} collected at five measurement sites in southern Italy. Atmos. 8, 243. https://doi.org/10.3390/atmos8120243.

EEAOC, 2020. Relevamiento de la superficie quemada en el área productiva de la provincia de Tucumán durante la campaña 2020. https://www.eeaoc.gob.ar/?publicacion=ra-202-relevamiento-de-la-supercie-quemada-en-el-area-productiva-de-la-provincia-de-tucuman-durante-la-campana-2020.

Fanizza, C., De Berardis, B., Ietto, F., Soggiu, M.E., Schirò, R., Inglessis, M., Ferdinandi, M., Incoronato, F., 2018. Analysis of major pollutants and physico-chemical characteristics of PM2. 5 at an urban site in Rome. Sci. Total Environ. 616, 1457-1468. https://doi.org/10.1016/j.scitotenv.2017.10.168.

García, M.E., Della Ceca, L.S., Micheletti, M.I., Piacentini, R.D.N., Ordano, M.A., Reyes, N.J., Buedo S., González, J.A., 2018. Satellite and ground atmospheric particulate matter detection over Tucumán city, Argentina, space-time distribution, climatic and seasonal variability. AIMS Environ. Sci. 5(3), 173-194. https://doi.org/10.3934/environsci.2018.3.173.

Grange, S.K., Uzu, G., Weber, S., Jaffrezo, J.L., Hueglin, C., 2022. Linking Switzerland's PM 10 and $PM_{2.5}$ oxidative potential (OP) with emission sources. Atmos. Chem. Phys. 22(10), 7029-7050. https://doi.org/10.5194/acp-22-7029-2022.

Hosseini, V., Shahbazi, H., 2016. Urban air pollution in Iran. Iranian Stud. 49(6), 1029-1046. https://doi.org/10.1080/00210862.2016.1241587.

Ji, D., Zhang, J., He, J., Wang, X., Pang, B., Liu, Z., Wang, L., Wang, Y., 2016. Characteristics of atmospheric organic and elemental carbon aerosols in urban Beijing, China. Atmos. Environ. 125, 293–306. https://doi.org/10.1016/j.atmosenv.2015.11.020.

Jordán, A.M., Flores, I., 2018. Efecto de la quema de caña en las consultas por patologías respiratorias y oculares de la población menor de 15 años en establecimientos públicos de salud de la provincia de Tucumán durante el periodo 2012-2015. https://msptucuman.gov.ar/wordpress/wp-content/uploads/2019/02/revista-cientifica-4-para-web.pdf.

Lee, H.H., Bar-Or, R.Z., Wang, C., 2017. Biomass burning aerosols and the low-visibility events in Southeast Asia. Atmos. Chem. Phys. 17(2), 965-980. https://doi.org/10.5194/acp-17-965-2017.

Li, Y.C., Yu, J.Z., Ho, S.S.H., Schauer, J.J., Yuan, Z., Lau, A.K.H., Louie, P.K.K., 2013. Chemical characteristics and source apportionment of fine particulate organic carbon in Hong

Kong during high particulate matter episodes in Winter. Atmos. Res. 120, 88–98. https://doi.org/10.1016/j.atmosres.2012.08.005.

Li, D., Yue, W., Gong, T., Gao, P., Zhang, T., Luo, Y., Wang, C., 2023. A comprehensive SERS, SEM and EDX study of individual atmospheric $PM_{2.5}$ particles in Chengdu, China. Sci. Total Environ. 883, 163668. https://doi.org/10.1016/j.scitotenv.2023.163668.

Liao, H.T., Lai, Y.C., Chao, H.J., Wu, C.F., 2023. Vertical characteristics of potential PM2. 5 sources in the Urban environment. Aerosol Air Qual. Res. 23(3), 220361. https://doi.org/10.4209/aaqr.220361.

Martínez Morales, S., Cerón Bretón, J.G., Carbajal, N., Cerón Bretón, R.M., Lara Severino, R., Kahl, J.D., Carrillo Ávila, J.R., Carranco Lozada, S.E., Espinosa Guzmán, A., Pech Pech, I.E., Garcia Martinez, R., Robles Heredia, J.C., Hernández López, G., Solís Canul, J.A., Uc Chi, M.P., 2023. $PM_{2.5}$-bound trace metals in an urban area of Northern Mexico during the COVID-19 pandemic: characterization, sources, and health risk. Air Qual. Atmos. Health, 16(9), 1789-1808. https://doi.org/10.1007/s11869-023-01372-7.

Mendez-Espinosa, J.F., Belalcazar, L.C., Betancourt, R.M., 2019. Regional air quality impact of northern South America biomass burning emissions. Atmos. Environ. 203, 131-140. https://doi.org/10.1016/j.atmosenv.2019.01.042.

Merkus, H.G., 2009. Particle size measurements, In: Valverde, M., José, M. (Eds.), Particle Technology Series. Springer, Netherlands. http://dx.doi.org/10.1007/978-1-4020-9016-5.

Mills, S.A., MacKenzie, A.R., Pope, F.D., 2024. Local spatiotemporal dynamics of particulate matter and oak pollen measured by machine learning aided optical particle counters. Sci. Total Environ.941, 173450. https://doi.org/10.1016/j.scitotenv.2024.173450.

Ministry of Environment and Sustainable Development, 2021. Informe del estado del ambiente 2020.https://www.argentina.gob.ar/sites/default/files/iea_2020_digital.pdf.

Pakbin, P., Hudda, N., Cheung, K.L., Moore, K.F., Sioutas, C., 2010. Spatial and temporal variability of coarse ($PM_{10-2.5}$) particulate matter concentrations in the Los Angeles area. Aerosol. Sci. Technol. 44, 514–525. https://doi.org/10.1080/02786821003749509.

Paisi, N., Kushta, J., Pozzer, A., Violaris, A., Lelieveld, J., 2024. Health effects of carbonaceous $PM_{2.5}$ compounds from residential fuel combustion and road transport in Europe. Sci. Rep. 14, 1530. https://doi.org/10.1038/s41598-024-51916-9.

Pandey, C.P., Negi, P.S., 2022. Characteristics of equivalent black carbon aerosols over Doon Valley in NW Indian Himalaya during COVID-19 lockdown 2020. Environ. Monit. Assess. 194(3), 229. https://doi.org/10.1007/s10661-022-09879-9.

Qonitan, F.D., Kuncoro, N.W., Rahman, A., Rahmi, S.A., Damayanti, S., 2023. Characterizing $PM_{2.5}$ Pollution in Urban Jakarta: Insights from Morphology, Elemental Composition, and Concentration Analysis. In: International Conference on Radioscience, Equatorial Atmospheric Science and Environment. Springer Nature Singapore, Singapore, pp. 87–99. https://doi.org/10.1007/978-981-97-0740-9_9.

Rausch, J., Jaramillo-Vogel, D., Perseguers, S., Schnidrig, N., Grobéty, B., Yajan, P., 2022. Automated identification and quantification of tire wear particles (TWP) in airborne dust: SEM/EDX single particle analysis coupled to a machine learning classifier. Sci. Total Environ. 803, 149832. https://doi.org/10.1016/j.scitotenv.2021.149832.

Sgrigna, G., Baldacchini, C., Esposito, R., Calandrelli, R., Tiwary, A., Calfapietra, C., 2016. Characterization of leaf-level particulate matter for an industrial city using electron microscopy and X-ray microanalysis. Sci. Total Environ. 548-549, 91-99. https://doi.org/10.1016/j.scitotenv.2016.01.057.

Shen, L., Wang, H., Kong, X., Yin, Y., Chen, K., Chen, J., 2021. Characterization of black carbon aerosol at the summit of Mount Tai (1534 m) in central east China: Temporal

variation, source appointment and transport. Atmos. Environ. 246, 118152.https://doi.org/10.1016/j.atmosenv.2020.118152.

Speranza, A., Caggiano, R., 2022. Impacts of the COVID-19 lockdown measures on coarse and fine atmospheric aerosol particles (PM) in the city of Rome (Italy): compositional data analysis approach. Air Qual. Atmos. Health, 15(11), 2035-2050. https://doi.org/10.1007/s11869-022-01235-7.

Tessum, M.W., Anenberg, S.C., Chafe, Z.A., Henze, D.K., Kleiman, G., Kheirbek, I., Marshall, J.D., Tessum, C.W., 2022. Sources of ambient $PM_{2.5}$ exposure in 96 global cities. Atmos. Environ., 286, 119234 .https://doi.org/10.1016/j.atmosenv.2022.119234.

Wang, F., Yu, H., Wang, Z., Liang, W., Shi, G., Gao, J., Li, M., Feng, Y., 2021. Review of online source apportionment research based on observation for ambient particulate matter. Sci. Total Environ. 762, 144095. https://doi.org/10.1016/j.scitotenv.2020.144095.

World Health Organization,2021. WHO global air quality guidelines: particulate matter ($PM_{2.5}$ and PM_{10}), ozone, nitrogen dioxide, sulfur dioxide and carbon monoxide: executive summary. https://apps.who.int/iris/handle/10665/345334.

Xu, H., Xiao, Z., Chen, K., Tang, M., Zheng, N., Li, P., Yang, N., Yang, W., Deng, X., 2019. Spatial and temporal distribution, chemical characteristics, and sources of ambient particulate matter in the Beijing-Tianjin-Hebei region. Sci. Total Environ. 658, 280–293. https://doi.org/10.1016/j.scitotenv.2018.12.164.

Yadav, R., Sahu, L.K., Beig, G., Tripathi, N., Jaaffrey, S.N.A., 2017. Ambient particulate matter and carbon monoxide at an urban site of India: influence of anthropogenic emissions and dust storms. Environ. Pollut. 225, 291-303. https://doi.org/10.1016/j.envpol.2017.01.038

Zangari, S., Hill, D.T., Charette, A.T., Mirowsky, J.E., 2020. Air quality changes in New York City during the COVID-19 pandemic. Sci. Total Environ. 742, 140496.

Zalakeviciute, R., Alexandrino, K., Rybarczyk, Y., Debut, A., Vizuete, K., Diaz, M., 2020. Seasonal variations in PM10 inorganic composition in the Andean city. Sci. Rep. 10(1), 17049. https://doi.org/10.1038/s41598-020-72541-2.

Zhao, P., Zhao, P., Tang, J., Casuccio, G.S., Gao, J., Li, J., He, Y., Li, M., Feng, Y., 2023. Source identification and apportionment of ambient particulate matter in Beijing using an advanced computer-controlled scanning electron microscopy (CCSEM) system. Sci. Total Environ. 861, 160608. https://doi.org/10.1016/j.scitotenv.2022.160608.

Zhou, J., Zhang, R., Cao, J., Chow, J.C., Watson, J.G., 2012. Carbonaceous and ionic components of atmospheric fine particles in Beijing and their impact on atmospheric visibility. Aerosol Air Qual. Res. 12(4), 492-502. https://doi.org/10.4209/aaqr.2011.11.0218.

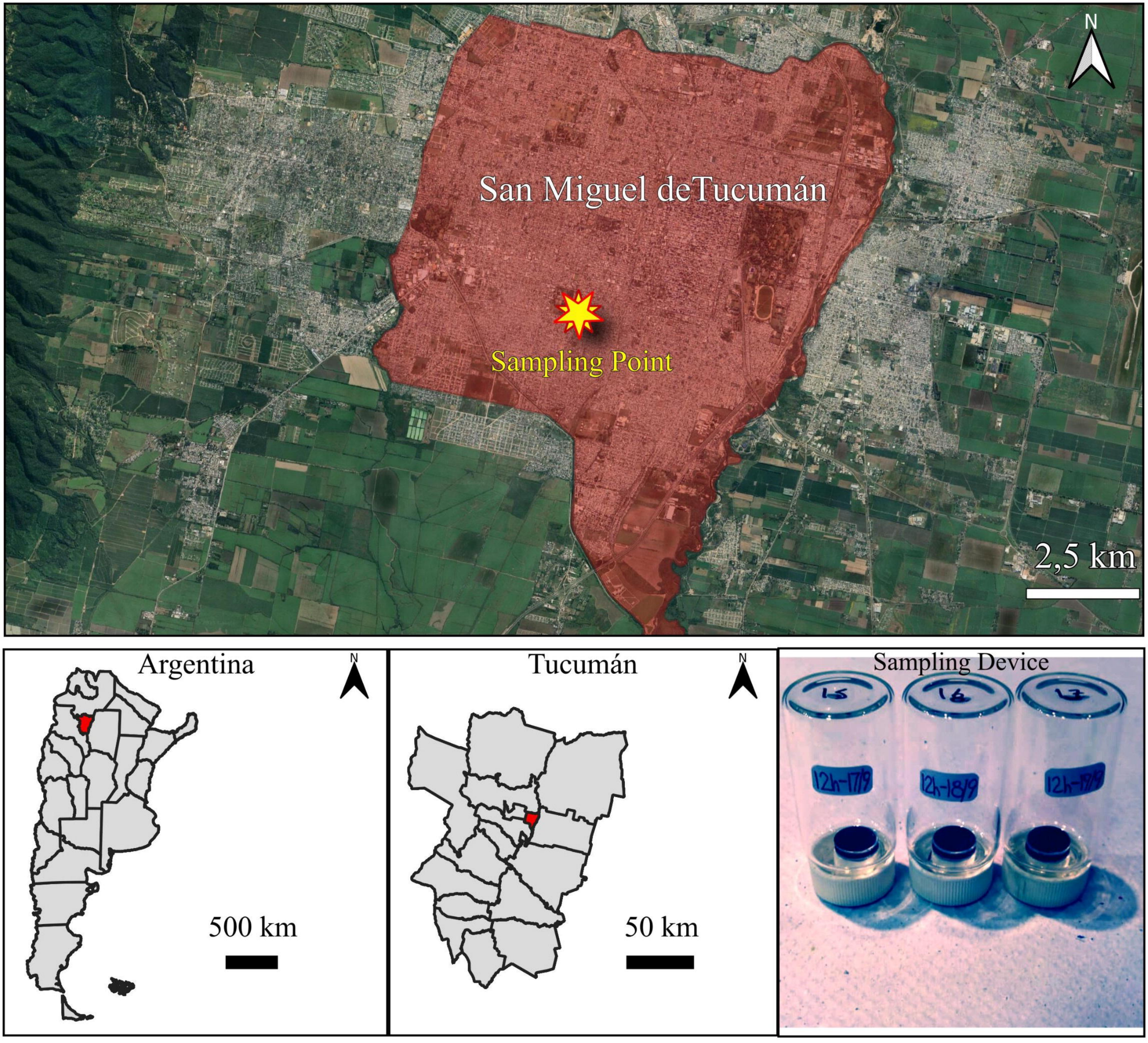
N
San Miguel deTucumán
Sampling Point
2,5 km
Argentina
N
500 km
Tucumán
N
50 km
Sampling Device
15
16
17
12h-17/9
12h-18/9
12h-19/9

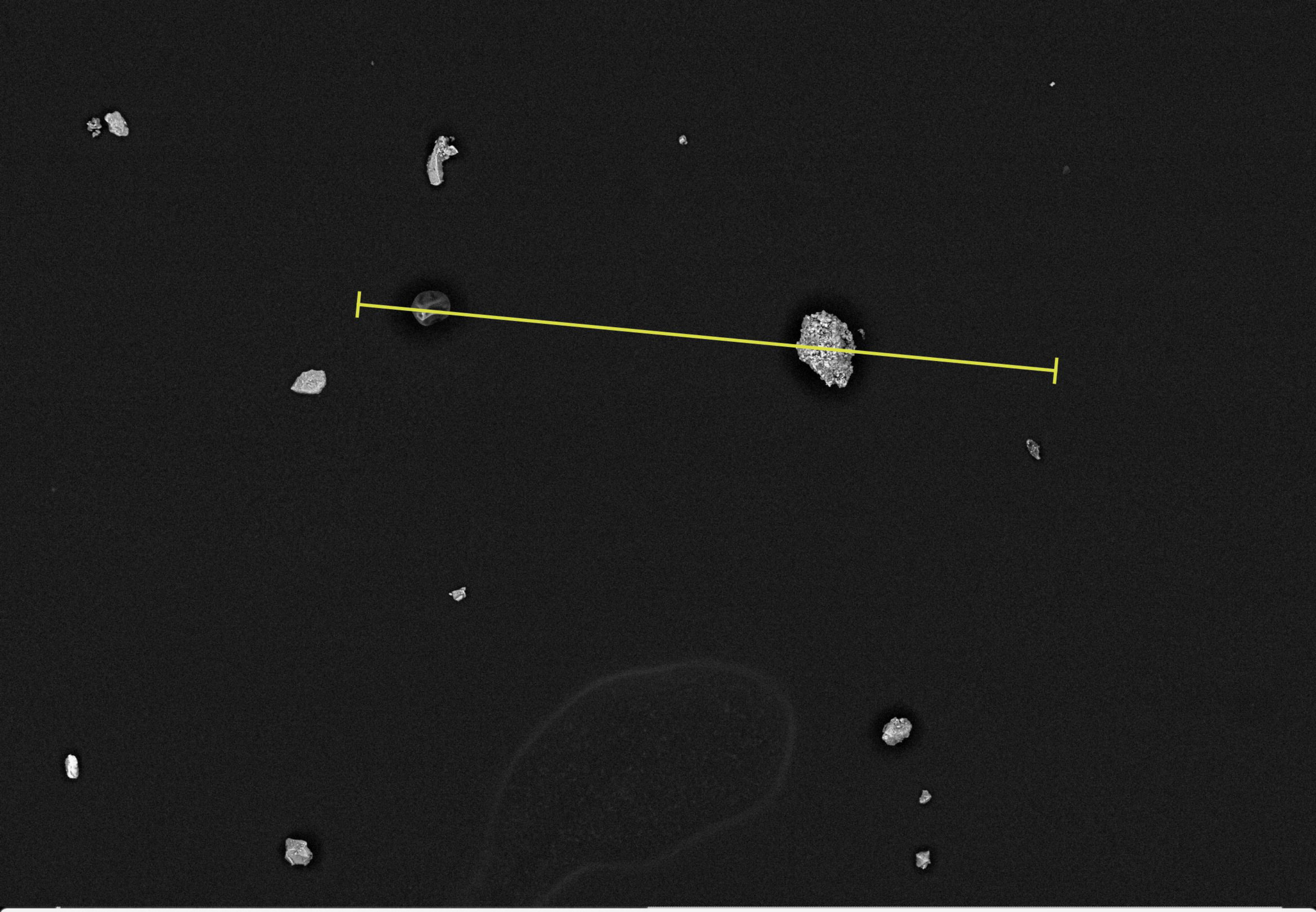

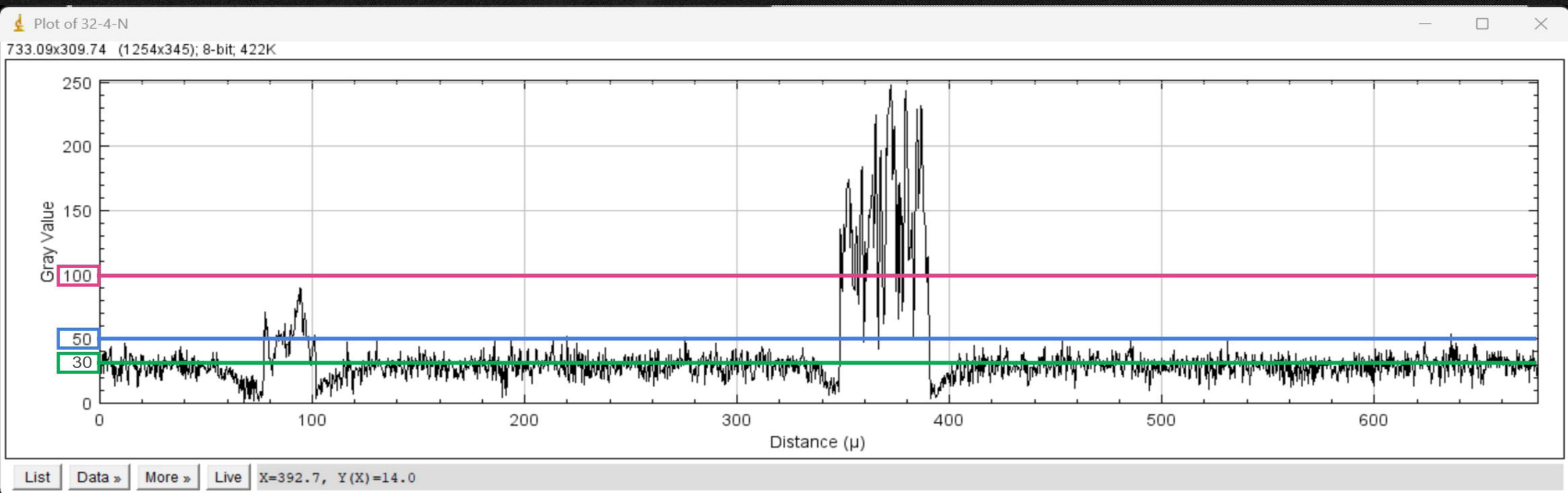
Plot of 32-4-N
733.09x309.74 (1254x345); 8-bit; 422K
Gray Value
250
200
150
100
50
30
0
0
100
200
300
400
500
600
Distance (µ)
List
Data »
More »
Live
X=392.7, Y(X)=14.0

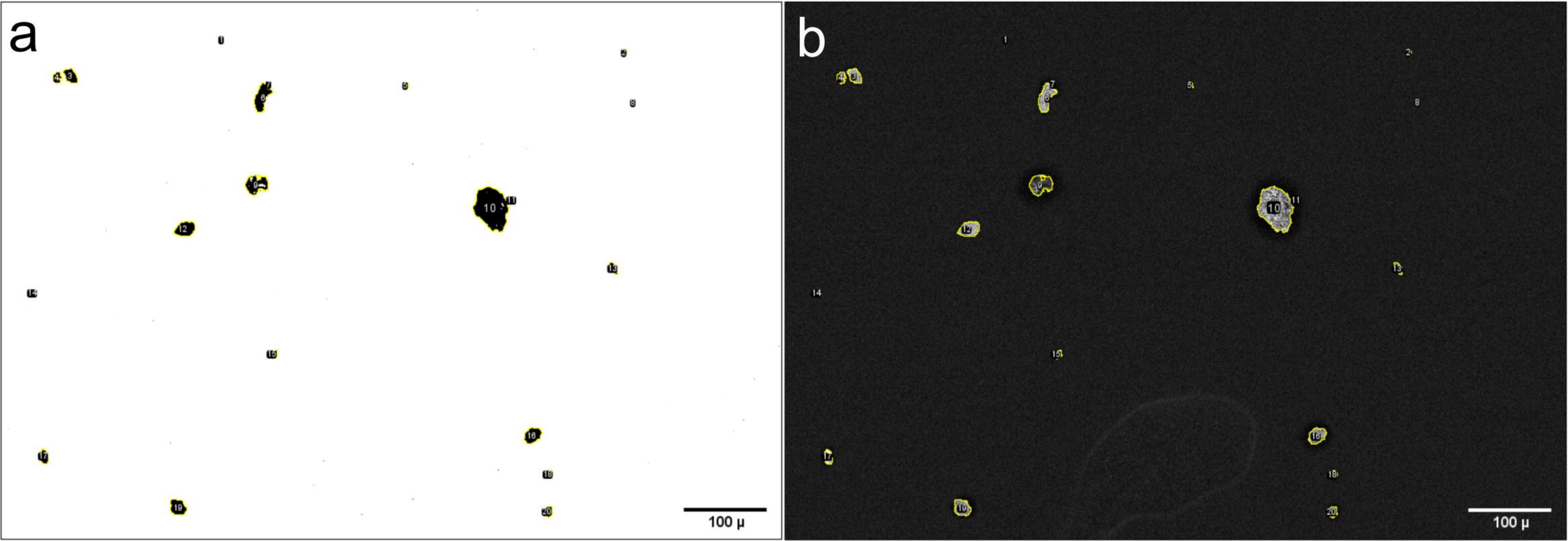
a
b
100 µ
100 µ

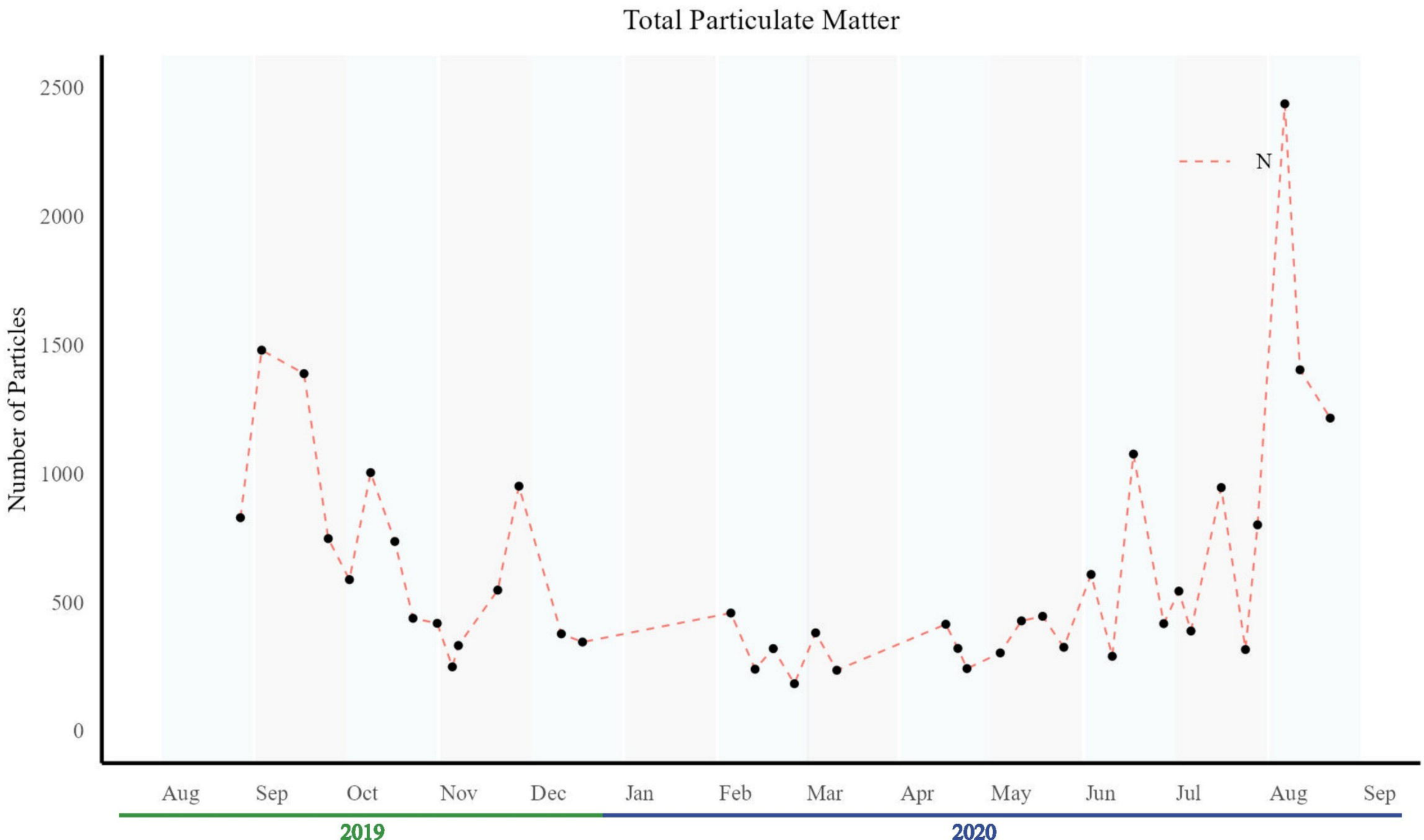
Total Particulate Matter
Number of Particles
2500
2000
1500
1000
500
0
N
Aug
Sep
Oct
Nov
Dec
Jan
Feb
Mar
Apr
May
Jun
Jul
Aug
Sep
2019
2020

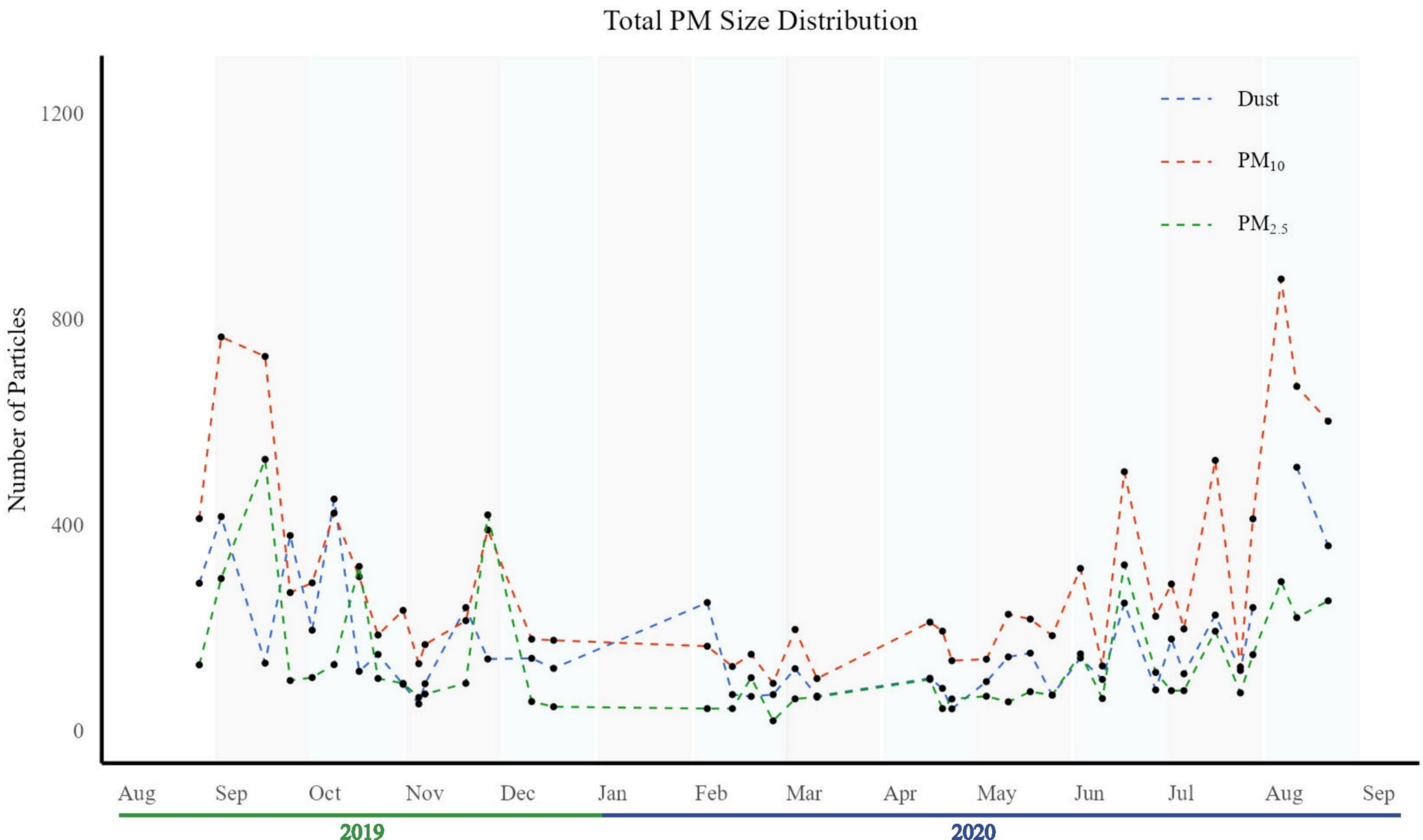
Total PM Size Distribution
Number of Particles
1200
800
400
0
Dust
PM10
PM2.5
Aug
Sep
Oct
Nov
Dec
Jan
Feb
Mar
Apr
May
Jun
Jul
Aug
Sep
2019
2020

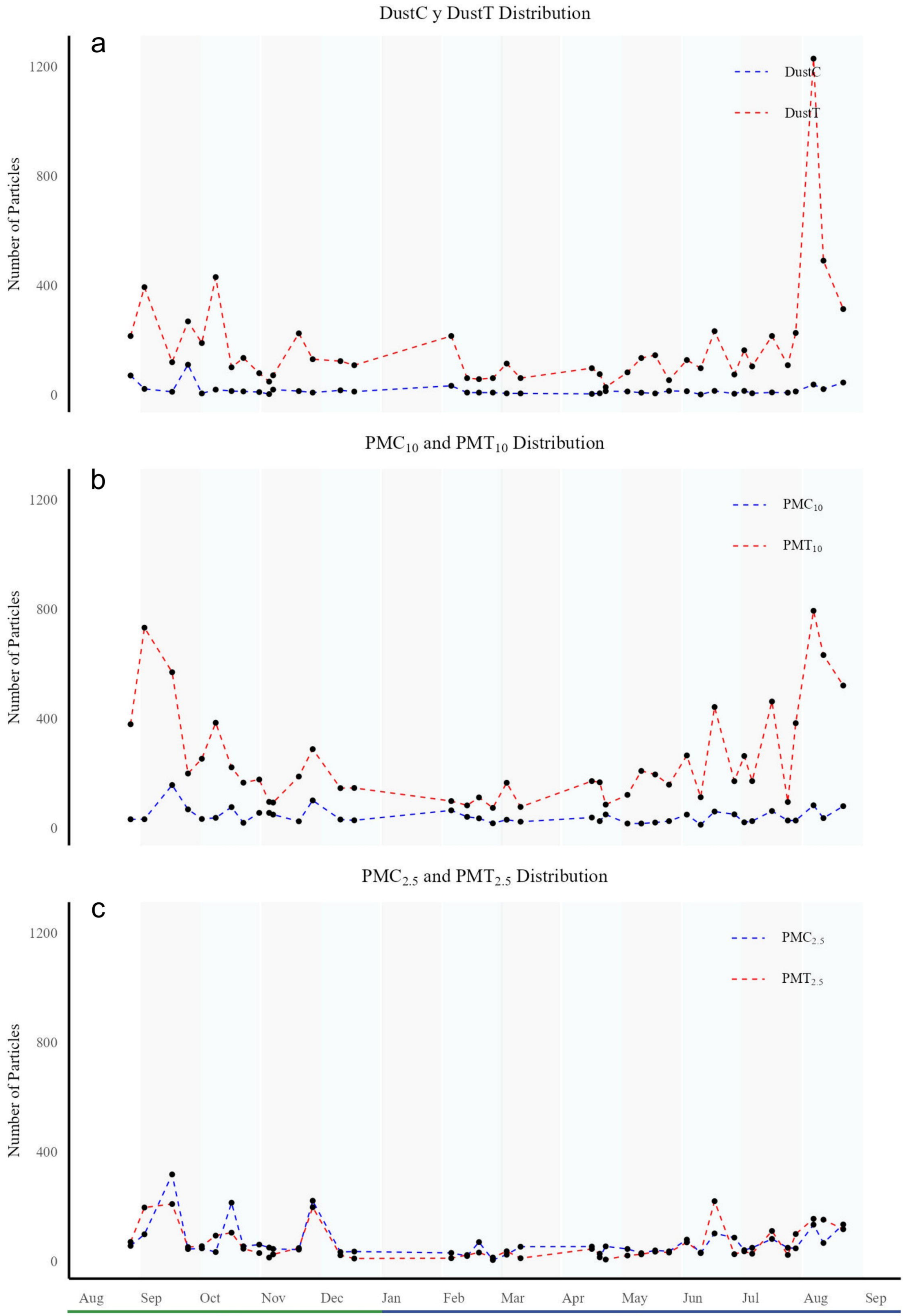
DustC y DustT Distribution
a
DustC
DustT
Number of Particles
1200
800
400
0
PMC10 and PMT10 Distribution
b
PMC10
PMT10
Number of Particles
1200
800
400
0
PMC2.5 and PMT2.5 Distribution
c
PMC2.5
PMT2.5
Number of Particles
1200
800
400
0
Aug
Sep
Oct
Nov
Dec
Jan
Feb
Mar
Apr
May
Jun
Jul
Aug
Sep
2019
2020

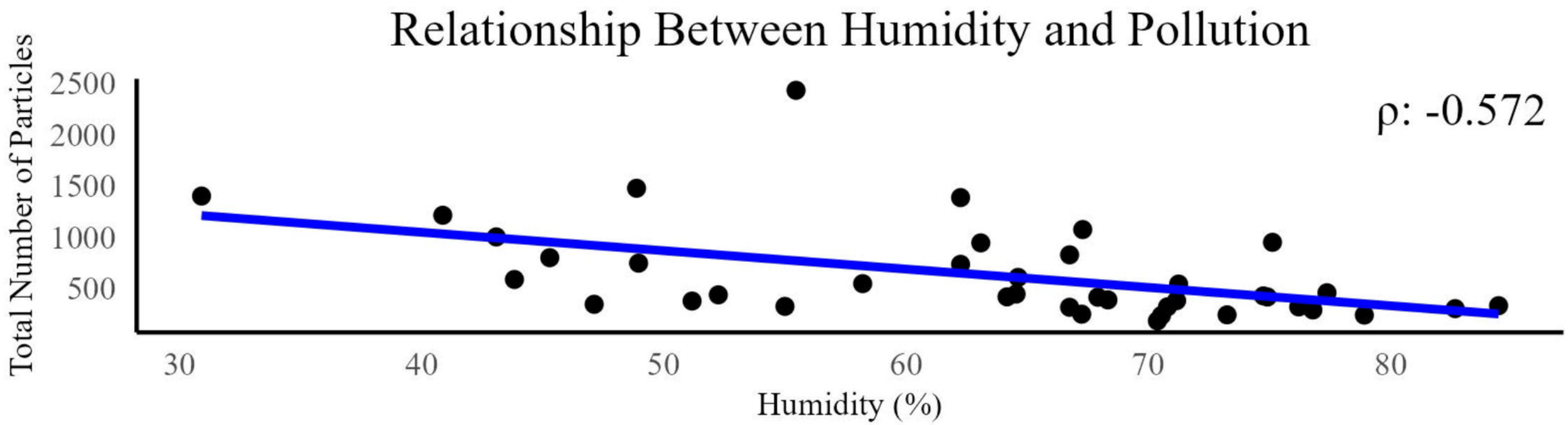
Relationship Between Humidity and Pollution
ρ: -0.572
Total Number of Particles
2500
2000
1500
1000
500
30
40
50
60
70
80
Humidity (%)

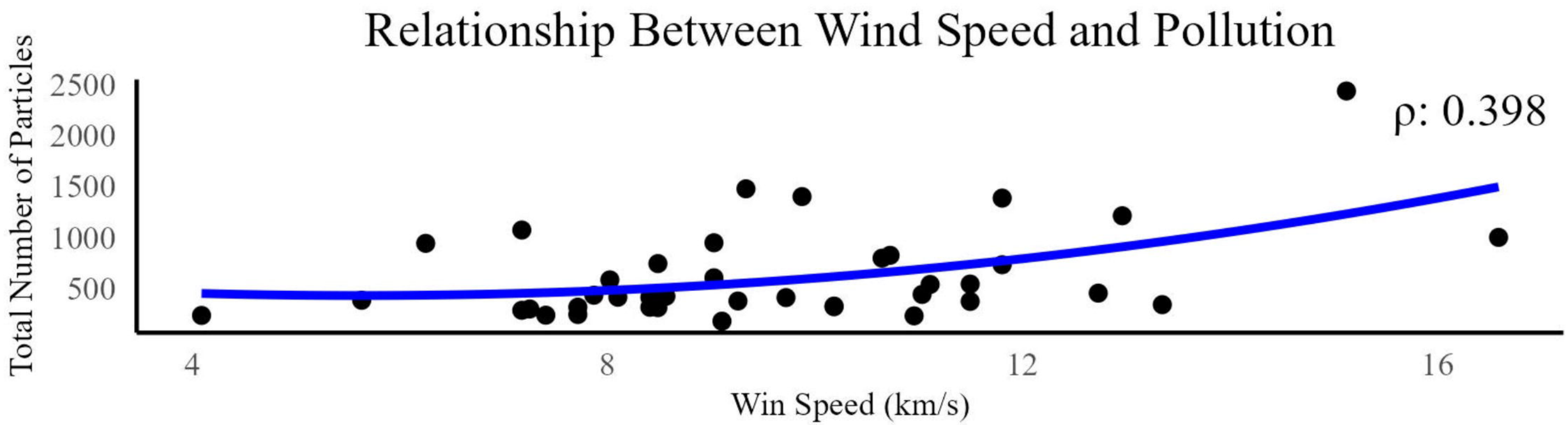
Relationship Between Wind Speed and Pollution
ρ: 0.398
Total Number of Particles
2500
2000
1500
1000
500
4
8
12
16
Win Speed (km/s)

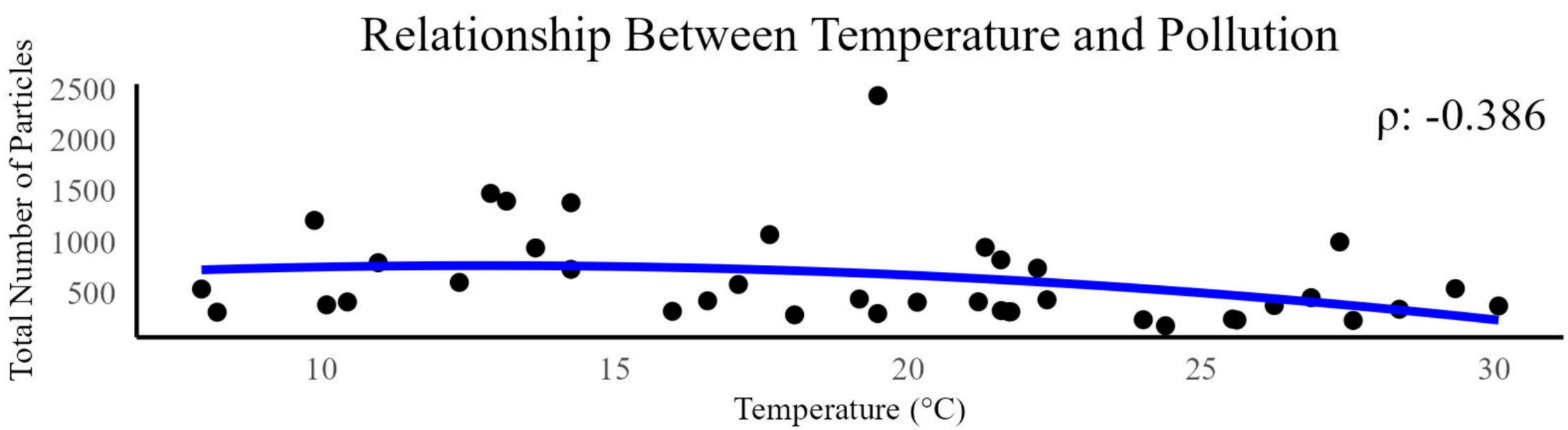
Relationship Between Temperature and Pollution
ρ: -0.386
Total Number of Particles
2500
2000
1500
1000
500
10
15
20
25
30
Temperature (°C)

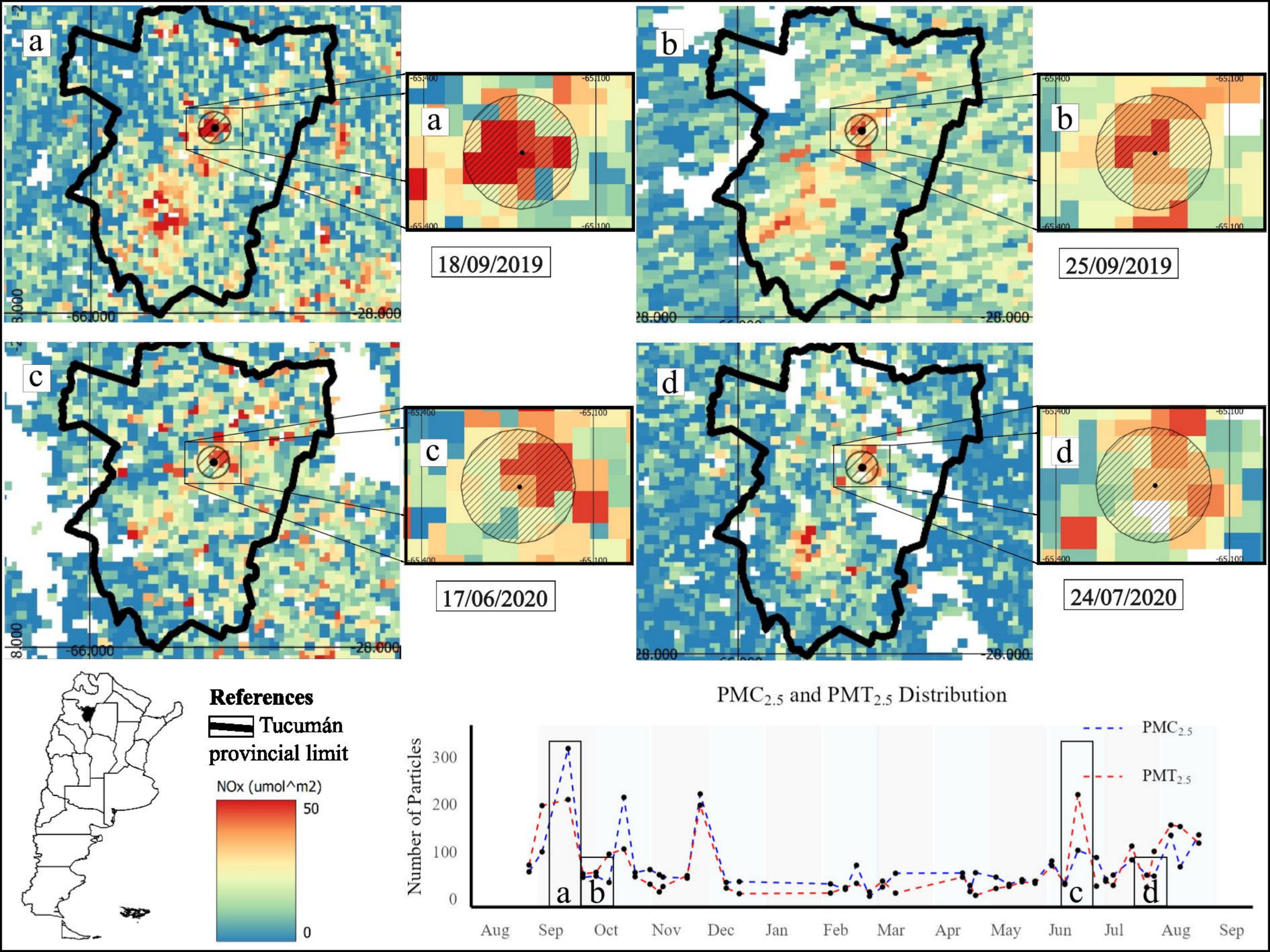
a
b
c
d
18/09/2019
25/09/2019
17/06/2020
24/07/2020
References
Tucumán provincial limit
NOx (umol^m2)
50
0
PMC2.5 and PMT2.5 Distribution
Number of Particles
300
200
100
0
PMC2.5
PMT2.5
Aug
Sep
Oct
Nov
Dec
Jan
Feb
Mar
Apr
May
Jun
Jul
Aug
Sep